ACSL3 As a Potential Prognostic Biomarker in Patients With Breast Cancer

Xiangyu Sun
The First Affiliated Hospital of China Medical University
Meng Li
The First Affiliated Hospital of China Medical University
Mozhi Wang
The First Affiliated Hospital of China Medical University
Mengshen Wang
The First Affiliated Hospital of China Medical University
Haoran Dong
The First Affiliated Hospital of China Medical University
Litong Yao
The First Affiliated Hospital of China Medical University
Xinyan Li
The First Affiliated Hospital of China Medical University
Yusong Wang
The First Affiliated Hospital of China Medical University
Shirong Tan
The First Affiliated Hospital of China Medical University
Yuhai Chen
the First Affiliated Hospital of China Medical University
Yingying Xu (xuyingying@cmu.edu.cn)
the First Affiliated Hospital of China Medical University https://orcid.org/0000-0003-0023-6841

Primary research

Keywords: Breast Cancer, LinkedOmics database, clinicopathological features, mammary tissues

Posted Date: January 6th, 2021

DOI: https://doi.org/10.21203/rs.3.rs-139587/v1

Abstract

Objective: To explore the expression pattern of long chain fatty acyl CoA synthetase 3 (ACSL3) in breast cancer, and evaluate the clinical significance of ACSL3 by analyzing potential function and prognostic value of ACSL3 in human breast carcinoma.

Methods: The expression of ACSL3 in normal mammary tissues and breast tumor tissues was analyzed by GEPIA and Human Protein Atlas. The prognostic value of ACSL3 was evaluated by Kaplan–Meier plotter analysis. ACSL3 expression was analyzed by immunohistochemistry in 297 breast cancer patients from the First Hospital of China Medical University Furthermore, based on LinkedOmics database, analyses of GO and KEGG pathways were performed to identify the potential function of ACSL3. Tumor Immune Estimation Resource (TIMER) database was used to evaluate the association between ACSL3 and immune infiltration in breast cancer.

Results: GEPIA and Human Protein Atlas indicated that ACSL3 was significantly upregulated in breast carcinomas. Kaplan-Meier plotter analysis showed that increased expression of ACSL3 mRNA was significantly associated with shorter overall survival (OS) and relapse-free survival (RFS) in breast cancer patients. Results from immunochemical staining showed that ACSL3 was obviously related to clinicopathological features of breast cancer, and ACSL3 was highly abundant in TNBC tumors. Moreover, survival analysis of breast cancer patients demonstrated that higher ACSL3 protein expression is unfavorable prognostic biomarker in breast cancer patients. Results from TIMER database indicated that ACSL3 expression was significantly correlated with infiltration level of multiple immune cells. Further studies are needed to explore underlying mechanism of the pro-tumor effects of ACSL3 expression.

Conclusions: ACSL3 may not only serve as a reliable predictive biomarker of breast cancer but also have impact on the occurrence and progression of breast cancer. Thus, ACSL3 may be an emerging therapeutic target for the development of molecular-targeted therapeutic strategies for breast cancer.

Introduction

Among females, breast cancer is the most commonly diagnosed cancer and the leading cause of death from cancer [1]. According to cancer statistics in 2020, nearly 279,100 new cases were diagnosed with breast cancer, leading to 42,690 deaths in the United States [2]. According to the status of the estrogen receptor (ER), progesterone receptor (PR) and human epidermal growth factor receptor 2 (HER2), breast cancer is divided into four intrinsic subtypes, namely luminal A, luminal B, HER2-positive, and triple-negative breast cancer (TNBC). Currently, the predominant therapeutic strategies for breast cancer includes surgical approach, chemotherapy and radiation treatment, which significantly enhance the therapeutic effects and improve the clinical outcome of patient diagnosed with breast cancer [3]. Although the advanced diagnostic methods and therapeutic means have been developed, the prognosis for some breast cancer patients are still poor. Thus, exploring for potential prognostic biomarkers to predict clinical outcomes of breast cancer patients with high sensitivity and specificity is an urgent need.

Metabolic reprogramming is an emerging hallmark of cancer cells [4]. Dysregulated lipid metabolism is a crucial component of metabolic adaption emerged in cancer cells. This metabolic adaptation includes not only sustained fatty acid uptake from the circulation and enhanced lipogenesis, but also elevated fatty acid oxidation within mitochondria [5,6]. Long chain fatty acyl CoA synthetase (ACSL) enzymes play crucial roles in the regulation of intracellular fatty acid metabolism through utilizing Co-enzyme A (CoA) and ATP to convert fatty acids to fatty acyl CoA [7]. ACSL-dependent fatty acid activation is an important preparation for the following metabolic pathways required by cell survival. Currently, five members of ACSL family (ACSL1-5 and ACSL6) have been identified in humans [8]. These isoforms display divergent substrate preferences and tissue specificity, therefore leading to different functional mechanisms [9]. Notably, ACSL3 is localized to the surfaces of lipid droplets and the endoplasmic reticulum, with the distribution dependent on the cell type and the supply of fatty acids. ACSL3 prefers substrates like palmitate and arachidonate, and regulates the production of constituent parts of lipid droplets including triacylglycerols and neutral lipids [8]. Considering the fact that lipid droplets biogenesis is crucial for cancer development, ACSL3 is an emerging therapeutic target for cancer treatment [10]. ACSL3 expression has been found to be significantly elevated in lung, liver, prostate cancer and melanoma, making ACSL3 a potential prognostic target for multiple cancer types [10-14]. However, ACSL3 expression in specimens from patients with breast carcinomas has not been extensively investigated.

Accordingly, in this study, we aimed to explore ACSL3 expression in breast tumors and to reveal the associations between ACSL3 protein and clinicopathological features or prognosis in breast cancer patients. Furthermore, we analyzed related functional regulatory network of ACSL3 and comprehensively evaluated the correlation between ACSL3 and immune infiltration level. Our findings are expected to help elucidate the mechanisms of breast cancer progression and to establish ACSL3 as a reliable prognostic factor and therapeutic target.

Materials And Methods

GEPIA analysis

GEPIA analysis is an interactive website for exploring the differential transcription expression of 9,736 tumors and 8,587 normal samples derived from TCGA [15]. The transcriptional expression of ACSL3 in cancerous and para-cancerous tissues of breast cancer were evaluated by GEPIA analysis. Threshold was defined as P value, 0.05.

Kaplan–Meier plotter analysis

Kaplan–Meier (KM) plotter analysis provides survival information of query genes in various cancer types [16]. The prognostic impact of ACSL3 was evaluated by Kaplan–Meier plotter by showing relapse free survival (RFS) and overall survival (OS). In the present study, we specifically selected the best probe set of ACSL3. Threshold was set as P value, 0.05.

LinkedOmics analysis

The LinkedOmics database is comprehensive web resource for analyzing datasets from 32 TCGA cancer types [17]. The LinkFinder module generates differentially expressed genes that associated with query gene, which can be visualized in the form of volcano plots, scatter plots or heat maps. The results derived from LinkedOmics were further analyzed by Web-based Gene SeT AnaLysis Toolkit (WebGestalt) to perform analyses of Gene Ontology (GO) including cellular component (CC), biological process (BP) and molecular function (MF), and KEGG pathways based on GSEA methods. The rank criterion was defined as FDR, 0.05; simulations, 500.

TIMER Analysis

TIMER is a publicly available resource for systematical analysis of immune infiltration level in various cancer types [18]. The immune infiltrates primarily include CD8 + T cells, CD4 + T cells, macrophages, neutrophils and B cells. The association between immune infiltrates and ACSL3 expression was analyzed in this webserver to explore tumor immunological, clinical and genomic features comprehensively.

Patients and Paraffin-embedded Tissue Samples

A total of 297 tissue samples from breast cancer patients were collected after surgery from the First Hospital of China Medical University from December 2014 to February 2016. All of the patients were diagnosed clearly by pathology with complete clinical data and follow-up data. Patients diagnosed with other malignant tumors were excluded.

Immunohistochemistry

Breast specimens were collected from the Department of Pathology at the First Hospital of China Medical University. The immunoreactivity of ACSL3 was scored based on both intensity of staining (negative = 0, weak = 1, moderate = 2, strong = 3) and percentage of positive tumor cells (<5% = 0, 5-25% = 1, 25-50%=2, 50-75% = 3, >75%=4). The final score was calculated by multiplying the single scores obtained from the intensity and percentage of positive cells (ranging from 0 to 12). The median expression score of ACSL3 was 4, which could be used as a cut-off value. Then patients with a score of at least 4 being applicable to the ACSL3 high expression population. Two pathologists independently examined the sections.

Statistical Analysis

Data analysis was implemented depending on SPSS version 19.0. The relevance between ACSL3 expression and clinic-pathological characteristics of breast cancer patients was examined by Chi-square test. Survival analysis of patients with breast cancer was calculated with KM plotter analysis. The Cox model was used to perform univariate and multivariate analyses.

Results

The expression level and prognostic value of ACSL3 in patients with breast cancer

The transcriptional level of ACSL3 was evaluated from GEPIA. The mRNA expression level of ACSL3 was significantly higher in breast cancer than that in normal tissues ($P < 0.05$) (Fig.1A). The ACSL3 expression in different tumor types from the TCGA database was also analyzed in GEPIA database. The results showed that mRNA expression was obviously elevated in BRCA (breast invasive carcinoma), CESC (cervical squamous cell carcinoma and endocervical adenocarcinoma), COAD (colon adenocarcinoma), DLBC (lymphoid neoplasm diffuse large B-cell lymphoma), PAAD (pancreatic adenocarcinoma), PRAD (prostate adenocarcinoma), READ (rectum adenocarcinoma), SKCM (skin cutaneous melanoma) and THYM (thymoma) tissues compared with the adjacent normal tissues. In contrast, mRNA expression was downregulated in LAML (acute myeloid leukemia) (Fig.1B). Next, the Kaplan–Meier Plotter was used to examine the prognostic values of the ACSL3 mRNA expression in breast cancer. Elevated mRNA expression of ACSL3 was correlated with a worse prognosis of RFS (Fig 1C, HR =1.14, 95% CI: 1.03–1.28, P=0,015). Next, we explored the correlation between ACSL mRNA expression and overall survival OS. Upregulated ACSL3 mRNA expression level suggested poor OS (Fig 1D, HR =1.26, 95% CI: 1.02–1.56, P=0.033). Next, based on the immunohistochemistry results from Human Protein Atlas database, we examined the expression of ACSL3 protein expression in breast cancer tissues and normal mammary tissues. The results revealed that ACSL3 protein was mainly located to the cell membrane and cytoplasm. Breast cancer tissues showed moderate to high ACSL3 expression, while non-cancerous tissues were detected moderate ACSL3 expression in adipocytes, glandular cells and myoepithelial cells (Fig 1E-F).

Validation of ACSL3 protein expression by IHC

We further evaluated the association between ACSL3 expression and the clinicopathological parameters in breast carcinomas. 297 patients diagnosed with breast carcinomas and underwent surgical excision were included. During the follow-up period, 42 cases have tumor progression (14.1%), contributing to 38 cases of deaths (12.8%). The median survival time was 63 months (varying from 14 to 69 months), and the median age at diagnosis of patients was 55 years (ranging from 27 to 83 years). In the study cohort, 75 (25.3%) were diagnosed as Luminal A subtype, 156 (52.5%) were diagnosed as Luminal B subtype, 23 (7.7%) as HER2-enriched subtype, and 43 (14.5%) as TNBC. A total of 251 cases with low and moderate pathological grade (I-II) and 46 cases of tumors with high pathological grade (III). A total of 179 (60.3%) patients had lymph node metastasis and 118 (39.7%) patients had no lymph node metastasis.

A total of 297 cases of breast cancer tissues were categorized into low and high ACSL3 expression groups. High ACSL3 expression was observed in 52.5% (156/297) of all cases. Immunochemical staining for different scores (0–3) was displayed in Figure 1A-D. Clinicopathologic characteristics are displayed in Table 1. ACSL3 expression was associated with ER expression, PR expression, different molecular subtype, histological grade, lymph node metastasis and tumor-node-metastasis (TNM) stage ($P < 0.05$). There were no statistically differences between ACSL3 expression and age at diagnosis, tumor size, HER2 expression and Ki67 ($P > 0.05$).

Relevance between ACSL3 expression and the status of ER, PR, and HER2

Next, we analyzed the results from immunochemical staining and clinicopathologic features of all patients to explore the relevance between ACSL3 protein expression and the status of ER, PR and HER2. Representative images of negative/positive status of ER, PR and HER2 were displayed in Figure 3A. We further combined semi-quantitative methods to calculate the difference. As illustrated in Figure 3B, ACSL3 were significantly upregulated in ER-compared to ER+ breast tumors (P <0.0001). Similar result was found in PR- compared to PR+ breast tumors (P <0.0001). However, no significant differences were found in the HER2 status (P =0.1106) of breast tumors. Collectively,

ASCL3 expression was significantly correlated with the status of hormone receptor.

Correlation between ACSL3 and molecular subtypes of breast carcinoma

We further investigated the relevance of ACSL3 expression and molecular subtypes of breast cancer.

Figure 4A manifested the representative images of ACSL3 immunochemical staining in luminal and TNBC subtypes. Further semi-quantitative analyses revealed that ACSL3 was significantly upregulated in TNBC tissues in comparison of luminal subtypes (P = 0.0034) (Figure 4B). No other significant differences were found within other disparate subtypes. Ultimately, we concluded that ACSL3 was relatively abundant in highly malignant TNBC tissues compared with luminal-subtype tissues.

High ACSL3 Protein Predicted Poor Prognosis of Breast Cancer Patients

Hazard ratio (HR) and 95% confidence interval (CI) were used to calculate the prognostic value of ACSL3 expression in patients diagnosed with breast cancer patients. Results from KM plotter analysis manifested that higher ACSL3 protein levels were significantly correlated with poor DFS (P = 0.002; HR = 0.332; 95% CI = 0.163-0.618) and OS (P = 0.002; HR = 0.283; 95% CI = 0.130–0.618) (Figure 5A-B). Higher levels of lymph node metastasis were found to be significantly correlated with poor DFS (P = 0.001; HR = 0.198; 95% CI = 0.078-0.503) and OS (P = 0.001; HR = 0.165; 95% CI = 0.058-0.464) (Figure 5C-D). Results from univariate Cox proportional hazard regression analysis in Table 2 and 3 disclosed that high histological grade, high Ki67 index, high lymph node metastasis and high expression of ACSL3 were significant correlated with worse DFS and OS for breast cancer patients. Further multivariate analysis revealed that high Ki67 index, high lymph node metastasis and ACSL3 high-expression were independent predictors of unfavorable DFS and OS. The relevance between ACSL3 expression and the prognosis in different molecular subtypes of breast cancer was further analyzed. ACSL3 protein expression showed a significant relevance between high ACSL3 expression and shorter OS in Luminal-type patients (P = 0.033; HR = 0.293; 95% CI = 0.094–0.908) (Figure 6A), while no significant correlation was found in HER2-enriched (P = 0.226; HR = 3.025; 95% CI = 0.504–18.143) and TNBC patients (P = 0.073; HR = 0.157; 95% CI = 0.021–1.186) (Figures 6B-C). KM plotter analysis of breast cancer patients with lymph node metastasis was further applied to evaluate the prognostic value of ACSL3 in breast cancer. In the positive lymph node metastasis group, higher ACSL3 protein level was associated with worse DFS [HR = 0.077 (0.018–0.323), P < 0.0001; Figure 7A] and OS [HR = 0.041 (0.006–0.305), P = 0.002; Figure 7B]. However, no relevance was observed in the negative lymph node metastasis group (Figure 7C-D).

Enrichment analysis of ACSL3 functional networks in breast cancer

The Function module of LinkedOmics was implemented to examine mRNA sequencing data from 1097 BRCA patients in the TCGA. As illustrated in Figure 8A, there were 4177 genes represented by dark red dots, displaying a significant positive relevance with ACSL3, while there were 5796 genes, represented by dark green dots, having a significant negative correlation with ACSL3 (false discovery rate [FDR] < 0.001). The top 50 significant genes that were positively and negatively associated with ACSL3 have been manifested in the heat map (Figure 8B-C). AS shown in statistical scatter plots (Figure 8D-F), ACSL3 expression displayed a strong positive relevance with expression of CUL3 (Pearson correlation = 0.4799, p = 4.775e−64), NDUFS1 (Pearson correlation = 0.4578, p = 9.759e−58), and TRIP12 (Pearson correlation =0.4364, p = 4.779e−52).

GO and KEGG analysis of ACSL3-related co-expressed genes in breast cancer

Based on these results, we applied significant GO term analysis by gene set enrichment analysis (GSEA). The biological process they participate primarily in cargo loading into vesicle (GO:0035459), Golgi vesicle transport (GO:0048193), protein localization to Golgi apparatus (GO:0034067), endomembrane system organization (GO:0010256), vacuolar transport (GO:0007034). Molecular function analysis showed enrichment in helicase activity (GO:0004386), ubiquitinyl hydrolase activity (GO:0070003), electron transfer activity (GO:0101005), ubiquitin-like protein transferase activity (GO:0019787), ATPase activity (GO:0016887) and double-stranded RNA binding (GO:0003725). Cellular Component analysis showed that genes differentially expressed in correlation with ACSL3 were enriched in the transcription elongation factor complex (GO:0008023), endoplasmic reticulum exit site (GO:0070971), tethering complex (GO:0099023), endoplasmic reticulum tubular network (GO:0071782) and Golgi-associated vesicle (GO:0005798). (Figure 9A–C). KEGG pathway analysis showed enrichment in the ubiquitin-mediated proteolysis (hsa04120), circadian rhythm (hsa04710), fatty acid biosynthesis (hsa00061), propanoate metabolism (hsa00640) and protein processing in endoplasmic reticulum (hsa04141) (Figure 9D).

Correlation analysis between ACSL3 expression and immune infiltration

The TIMER analysis was performed to comprehensively assess the correlations between ACSL3 expression and a panel of immune infiltrates in human breast cancer. As illustrated in Figure 10, ACSL3 expression was positively correlated with infiltration level of CD8 + T cells (r= 0.219, P=2.79e-12) and macrophages (r= 0.314, P=3.43e-24), while ACSL3 expression was negatively correlated with infiltration level of CD4 + T cells (r= -0.257, P=1.66e-16). No significant correlation with ACSL3 expression was found in B cells and neutrophils. The relationship between ACSL3 expression and immune infiltration was further analyzed according to molarcular subtypes. In both luminal subtypes of breast cancer, ACSL3 displayed the greatest correlation with macrophages (r= 0.31, P=5.80e-13; r= 0.222, P=1.95e-03). Besides, ACSL3 expression was positively correlated with infiltration level of CD8 + T cells (r= 0.288, P=2.43e-11; r= 0.145, P=4.53e-02) and neutrophil (r= 0.19, P=1.40e-05; r= 0.169, P=1.92e-02), while negatively correlated with infiltration level of CD4 + T cells (r=-0.312, P=3.77e-13; r= -0.158, P=2.86e-02) in both luminal subtypes of breast cancer. In HER2-positive breast cancer, ACSL3 showed significant correlation

with infiltration level of CD4 + T cells (r=-0.272, p=2.09e-02) and macrophages (r=0.291, p=1.33e-02). In basal-like breast cancer, ACSL3 was significantly correlated with infiltration level of macrophages (r=0.234, p=1.90e-03) and B cell (r=-0.16, p=3.47e-02).

Discussion

The role of ACSL3 in the tumorigenesis has been extensively studied. Precious studies reported that ACSL3 was highly expressed in various cancer types. In prostate cancer, *ACSL3* serves as an androgen-responsive gene and participates in the production of fatty acyl-CoA esters [10]. Notably, ACSL3 has been found to be significantly upregulated in castration-resistant prostate cancer. ACSL3 gets involved in the upregulation of steroidogenesis-related genes to facilitate the proliferation of castration-resistant prostate cancer cells, making ACSL3 a candidate therapeutic target for castration-resistant cancer cell populations [12]. The essential role of ACSL3 in mutant KRAS lung cancer has also been illustrated in recent studies [19]. In mutant KRAS lung cancer, ACSL3 mediates the conversion of fatty acids into fatty Acyl-CoA esters to provide the substrates for lipid synthesis and β-oxidation, which can regulate intracellular fatty acid metabolism. Furthermore, ACSL3 also gets involved in channeling arachidonic acids into phosphatidylinositols to provide the lysophosphatidylinositol-acyltransferase 1 with a supplementation of arachidonic acids to promote sustained prostaglandin synthesis [20]. In pancreatic cancer, ACSL3 is highly expressed and closely related to enhanced fibrosis. Depletion of ACSL3 not only suppresses the development of pancreatic and reduces tumor fibrosis, but also enhances cytotoxic T cell infiltration and restrains immunosuppressive cells. These effects are partly resulted from reduced release of plasminogen activator inhibitor–1 from tumor cells [24]. In TNBC, CUB domain-containing protein 1 has been found to interact with ACSL3 and inhibits the activity of ACSL3, leading to restrained fatty acid utilization and enhanced fatty acid oxidation. This illustrates high fatty acid oxidation/low lipid droplet accumulation may be used to predict the metastatic potential of TNBC [21].

Breast cancer was generally characterized with poor immunogenicity and low mutation burden. Numerous evidences disclosed that higher T lymphocyte infiltration has been found in HER2 positive and TNBC subtypes compared to luminal-subtype [22-23]. Higher level of T lymphocyte infiltration within tumor microenvironment is correlated with a better prognosis in patients with early stage HER2 positive and TNBC subtypes [22]. There are a lot of challenges waiting for further exploration about the immune response of cancer with poor immunogenicity, especially in identifying potential therapeutic targets and improve the efficacy of immunotherapies in breast cancer. Based on the results from TIMER analysis, we found ACSL3 expression was positively correlated with infiltration level of CD8 + T cells and macrophages. Recent study found that ACSL3 suppression hinders the infiltration of immunosuppressive cell populations in tumors, including M2-like macrophages and Tregs in pancreatic cancer, while little is known about the role of ACSL3 in immune response of breast cancer [24]. Accumulating studies reported that dysregulated fatty acid metabolism displays complex interplay with the immune status. Thus, we speculated that the ACSL3-mediated metabolic reprogramming in breast tumor cells may contribute to the immune infiltration, which provokes further investigation of complex interplay between metabolic reprogramming and immune infiltration in breast carcinomas.

ACSL3 has been identified as a prognostic factor in some tumors. In the current study, ACSL3 expression was found to be associated with ER expression, PR expression, different molecular subtype, histological grade, lymph node metastasis and TNM stage. Further analysis on IHC score exposed that ACSL3 expression was distinctly correlated with ER and PR status. The connection between ACSL3 protein levels and the molecular subtypes of breast cancer was further explored, ACSL3 was relatively abundant in highly malignant TNBC specimens compared with luminal-type specimens. KM survival analysis revealed statistically significant correlations between higher expression of ACSL3 protein and poor DFS as well as OS. The underlying mechanism for the correlations may be related to the role of ACSL3 played in participation of metabolic rewiring in breast tumor cells. ACSL3 protein expression displays better prognostic effect in breast cancer with lymph node metastasis, which may have clinical implications for tumor managements of breast cancer patients with lymph node metastasis.

Conclusion

In the current study, ACSL3 was obviously related to clinicopathological features of breast cancer, and ACSL3 was highly abundant in TNBC tumors. Moreover, survival analysis of breast cancer patients demonstrated that higher ACSL3 protein expression is unfavorable prognostic biomarker in breast cancer patients. Further studies are needed to explore underlying mechanism of the pro-tumor effects of ACSL3 expression.

Declarations

Acknowledgements: Not applicable.

Authors' contributions: XS analyzed the collected data and wrote the first draft of the manuscript. ML wrote the first draft of the manuscript. MoW, MeW, HD, LY, XL, YW, ST and YC collected the data. YX supervised the whole project and prepared the final version of the manuscript. All authors have read and approved the manuscript.

Funding: This work was supported by National Natural Science Foundation of China (81773083), Scientific and Technological Innovation Leading Talent Project of Liaoning Province (XLYC1802108) and Support Project for Young and Technological Innovation Talents of Shenyang (RC190393). These projects provided all the funds necessary for the collection of cases, the analyses of results, the statistical interpretation of the data and for the submission of the manuscript.

Availability of data and materials: The datasets used and analyzed during the current study are available from the corresponding author upon request.

Ethics approval and consent to participate: This study was allowed by the Ethics Committee of the First Affiliated Hospital of China Medical University. All the participants signed an informed consent to participate in this study and a consent for the publication of the anonymized data has also been obtained.

Consent for publication Not applicable.

Competing interests: The authors declare that they have no competing interests.

References

1. Bray F, Ferlay J, Soerjomataram I, Siegel RL, Torre LA, Jemal A. Global Cancer Statistics 2018: GLOBOCAN Estimates of Incidence and Mortality Worldwide for 36 Cancers in 185 Countries. *CA Cancer J Clin*. 2018;68(6):394-424. doi: 10.3322/caac.21492
2. Siegel RL, Miller KD, Jemal A. Cancer statistics, 2020. *CA Cancer J Clin*. 2020; 70(1):7-30. doi: 10.3322/caac.21590
3. Waks AG, Winer EP. Breast Cancer Treatment. *JAMA*. 2019; 321(3):316. doi: 10.1001/jama.2018.20751
4. Pavlova NN, Thompson CB. The Emerging Hallmarks of Cancer Metabolism. *Cell Metab.* 2016; 23(1):27-47. doi: 10.1016/j.cmet.2015.12.006
5. Menendez JA, Lupu R. Fatty acid synthase and the lipogenic phenotype in cancer pathogenesis. *Nat Rev Cancer*. 2007; 7(10):63-77. doi: 10.1038/nrc2222
6. Ma Y, Temkin SM, Hawkridge AM, *et al*. Fatty acid oxidation: An emerging facet of metabolic transformation in cancer. *Cancer Lett.* 2018; 435:92-100. doi: 10.1016/j.canlet.2018.08.006
7. Ellis JM, Frahm JL, Li LO, Coleman RA. Acyl-coenzyme A synthetases in metabolic control. *Curr Opin Lipidol.* 2010; 21(3):212-7. doi: 10.1097/mol.0b013e32833884bb
8. Grevengoed TJ, Klett EL, Coleman RA. Acyl-CoA Metabolism and Partitioning. *Annu Rev Nutr.* 2014; 34:1-30. doi: 10.1146/annurev-nutr-071813-105541
9. Li LO, Klett EL, Coleman RA. Acyl-CoA synthesis, lipid metabolism and lipotoxicity. *Biochim Biophys Acta.* 2010; 1801(3):246-51. doi: 10.1016/j.bbalip.2009.09.024
10. Migita T, Takayama KI, Urano T, *et al*. ACSL3 promotes intratumoral steroidogenesis in prostate cancer cells. *Cancer Sci*. 2017; 108(10):2011-2021. doi: 10.1111/cas.13339
11. Ndiaye H, Liu JY, Hall A, Minogue S, Morgan MY, Waugh MG. Immunohistochemical staining reveals differential expression of ACSL3 and ACSL4 in hepatocellular carcinoma and hepatic gastrointestinal metastases. *Bioscience Rep.* 2020; 40(4): BSR20200219. doi: 10.1042/BSR20200219
12. Obinata D, Takayama K, Fujiwara K, *et al*. Targeting Oct1 genomic function inhibits androgen receptor signaling and castration-resistant prostate cancer growth. *Oncogene*. 2016;35(49):6350-58. doi: 10.1038/onc.2016.171
13. Wang J, Scholtens D, Holko M, *et al*. Lipid Metabolism Genes in Contralateral Unaffected Breast and Estrogen Receptor Status of Breast Cancer. *Cancer Prev Res.* 2013; 6(4):321-30. doi: 10.1158/1940-6207

14. Chen W, Wang C, Hung Y, et al. Systematic Analysis of Gene Expression Alterations and Clinical Outcomes for Long-Chain Acyl-Coenzyme A Synthetase Family in Cancer. *Plos One.* 2016;11(5):e0155660. doi: 10.1371/journal.pone.0155660
15. Tang Z, Li C, Kang B, Gao G, Li C, Zhang Z. GEPIA: a web server for cancer and normal gene expression profiling and interactive analyses. *Nucleic Acids Res.* 2017; 45(W1): W98-W102. doi: 10.1093/nar/gkx247
16. Nagy Á, Lánczky A, Menyhárt O, Győrffy B. Validation of miRNA prognostic power in hepatocellular carcinoma using expression data of independent datasets. Sci Rep. 2018;8(1):9227.
17. Vasaikar SV, Straub P, Wang J, Zhang B. LinkedOmics: analyzing multi-omics data within and across 32 cancer types. *Nucleic Acids Res.* 2018; 46(D1): D956-D963. doi: 10.1093/nar/gkx1090
18. Li T, Fan J, Wang B, et al. TIMER: A web server for comprehensive analysis of tumor-infiltrating immune cells. *Cancer Res*. 2017; 77: e108-10. doi: 10.1158/0008-5472.CAN-17-0307
19. Padanad MS, Konstantinidou G, Venkateswaran N, Melegari M, Rindhe S, Mitsche M, Fatty Acid Oxidation Mediated by Acyl-CoA Synthetase Long Chain 3 Is Required for Mutant KRAS Lung Tumorigenesis. *Cell Rep*. 2016; 16(6):1614-28. doi: 10.1016/j.celrep.2016.07.009
20. Saliakoura M, Reynoso-Moreno I, Pozzato C, *et al.* The ACSL3-LPIAT1 signaling drives prostaglandin synthesis in non-small cell lung cancer. *Oncogene.* 2020; 39(14):2948-60. doi: 10.1038/s41388-020-1196-5
21. Wright HJ, Hou J, Xu B, *et al.* CDCP1 drives triple-negative breast cancer metastasis through reduction of lipid-droplet abundance and stimulation of fatty acid oxidation. *Proc Natl Acad Sci U S A.* 2017; 114(32):E6556-E6565. doi: 10.1073/pnas.1703791114
22. Savas P, Salgado R, Denkert C, *et al.* Clinical relevance of host immunity in breast cancer: from TILs to the clinic. *Nat Rev Clin Oncol.* 2016; 13(4):228-41. doi: 10.1038/nrclinonc.2015.215.
23. Sugie T. Immunotherapy for metastatic breast cancer. *Chin Clin Oncol*. 2018;7(3):28. doi: 10.21037/cco.2018.05.05
24. Rossi Sebastiano M, Pozzato C, Saliakoura M, *et al*. ACSL3-PAI-1 signaling axis mediates tumor-stroma cross-talk promoting pancreatic cancer progression. *Sci Adv*. 2020;6(44):eabb9200. doi: 10.1126/sciadv.abb9200

Tables

Table 1 Correlation of ACSL3 expression with clinic-pathological parameters in patients with breast cancer.

Variables	Cases Number (%)	ACSL3 expression		*P* value
		Low	High	
Age at diagnosis				0.738
≤35	104 (35.0%)	48 (34.0%)	56 (35.9%)	
>35	193 (65.0%)	93 (66.0%)	100 (64.1%)	
Tumor size				0.632
≥ 3cm	11 (47.5%)	6 (4.3%)	5 (3.2%)	
< 3cm	286 (52.5%)	135 (95.7%)	151 (96.8%)	
Lymph node metastasis				**0.033**
no	118(39.7%)	65(46.1%)	53(34.0%)	
yes	179(60.3%)	76(53.9%)	103(66.0%)	
ER				**<0.0001**
Negative	224 (75.4%)	120 (85.1%)	104 (66.7%)	
Positive	73 (24.6%)	21 (14.9%)	52 (33.3%)	
PR				**0.006**
Negative	108 (36.4%)	40 (28.4%)	68 (43.6%)	
Positive	189 (63.6%)	101 (71.6%)	88 (56.4%)	
HER2				0.331
Negative	202 (68.0%)	92 (65.2%)	110 (70.5%)	
Positive	95 (32.0%)	49 (34.8%)	46 (29.5%)	
Ki67				0.641
Negative	66 (22.2%)	33 (23.4%)	33 (21.2%)	
Positive	231 (77.8%)	108 (76.6%)	123 (78.8%)	
Histological grade				**<0.0001**
0-I	251 (84.5%)	131 (92.9%)	120 (76.9%)	
II-III	46 (15.5%)	10 (7.1%)	36 (23.1%)	
Molecular subtype				**<0.0001**
Luminal A	75 (25.3%)	41 (29.1%)	34 (21.8%)	
Luminal B	156 (52.5%)	81 (57.4%)	75 (48.1%)	

Her-2	23 (7.7%)	8 (25.7%)	15 (9.6%)	
TNBC	43 (14.5%)	11(7.8%)	32 (20.5%)	
TNM staging				**0.004**
0-I	41 (13.8%)	28 (19.9%)	13 (8.3%)	
II-III	256 (86.2%)	113 (80.1%)	143 (91.7%)	

Table 2 Cox univariate analysis of OS and DFS in patients with breast cancer.

	OS			**DFS**		
	P-value	Exp(B)	HR (95%CI)	*P*-value	Exp(B)	HR (95%CI)
Expression of ACSL3 (Low vs high)	**0.002**	0.283	0.130 -0.618	**0.002**	0.332	0.163-0.618
Lymph node metastasis (No vs yes)	**0.001**	0.165	0.058-0.464	**0.001**	0.198	0.078-0.503
Tumor size (≥ 3cm vs < 3cm)	0.158	2.337	0.719 -7.600	0.176	2.253	0.694-7.309
Histological grade (0-I vs II-III)	**0.049**	0.484	0.235-0.997	**0.038**	0.482	0.242-0.960
Ki67 (≤14% vs >14%)	**0.019**	0.183	0.044 -0.760	**0.013**	0.167	0.040-0.689
TNM staging (I vs II-III)	0.071	0.160	0.022-1.167	0.057	0.146	0.020-1.062
Age at diagnosis (≤35 vs >35)	0.321	0.772	0.728-2.638	0.356	1.337	0.721-2.479

Table 3 Cox multivariate analysis of OS and DFS in patients with breast cancer.

	OS			DFS		
	P-value	Exp(B)	HR (95%CI)	*P*-value	Exp(B)	HR (95%CI)
Expression of ACSL3 (Low vs high)	**0.013**	0.364	0.164-0.808	**0.022**	0.427	0.206-0.884
Lymph node metastasis (No vs yes)	**0.007**	0.205	0.064-0.653	**0.010**	0.260	0.093-0.726
Tumor size (≥ 3cm vs < 3cm)	0.525	1.491	0.436-5.099	0.522	1.493	0.438-5.092
Histological grade (0-I vs II-III)	0.278	0.664	0.316-1.391	0.189	0.622	0.307-1.263
Ki67 (≤14% vs >14%)	**0.020**	0.183	0.044-0.766	**0.013**	0.164	0.039-0.683
TNM (I vs II-III)	0.797	0.747	0.081-6.884	0.570	0.532	0.060-4.683
Age at diagnosis (≤35 vs >35)	0.434	1.306	0.669-2.548	0.470	1.267	0.668-2.403

Figures

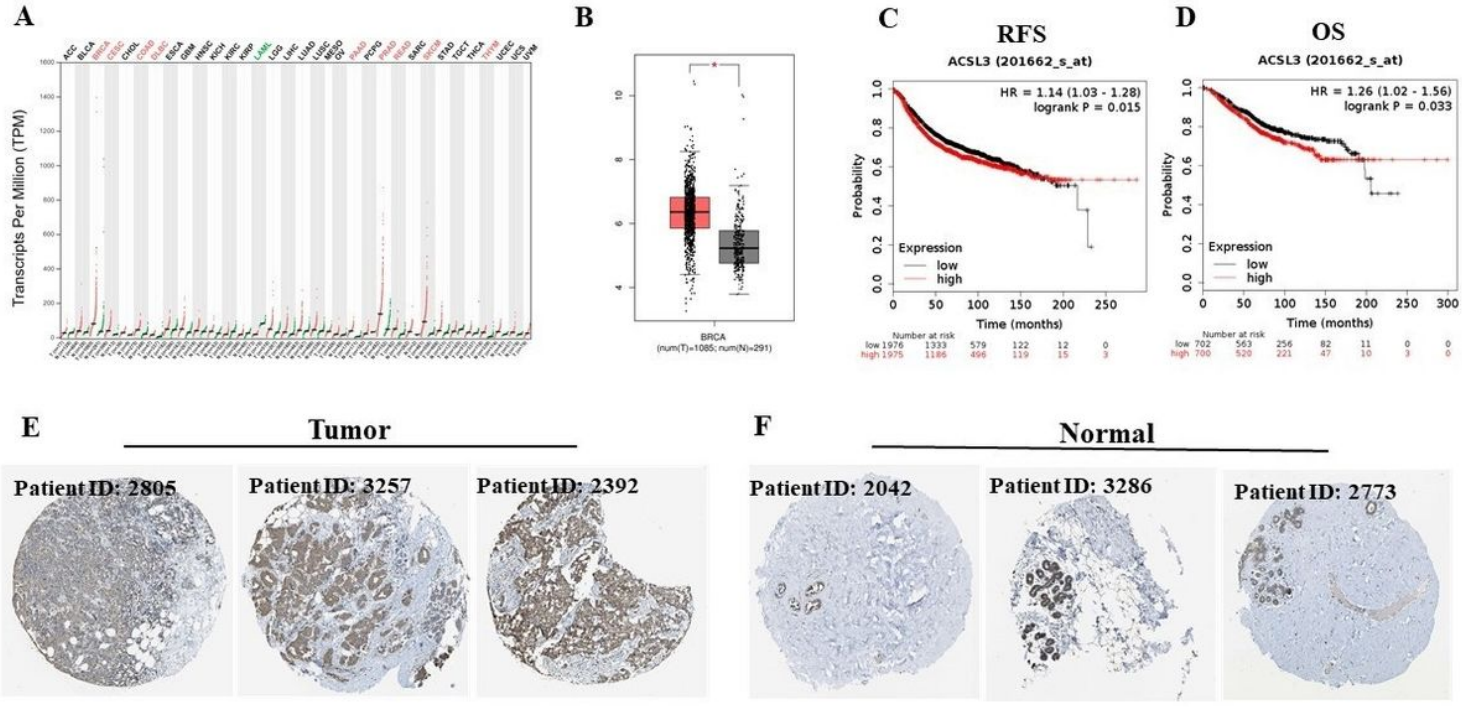

Figure 1

The expression and prognostic values of ACSL3 in breast cancer (GEPIA, Kaplan–Meier plotter and Human Protein Atlas). (A) the transcriptional level of ACSL3 in multiple cancer types. (B) the ACSL3 mRNA expression in breast cancer. (C) the relationship between the expression of ACSL3 and RFS in patients with breast cancer. (D) the relationship between the expression of ACSL3 and OS in patients with breast cancer. (E) the ACSL3 protein expression in breast tumor tissues from Human Protein Atlas. (F) the ACSL3 protein expression in breast normal tissues from Human Protein Atlas.

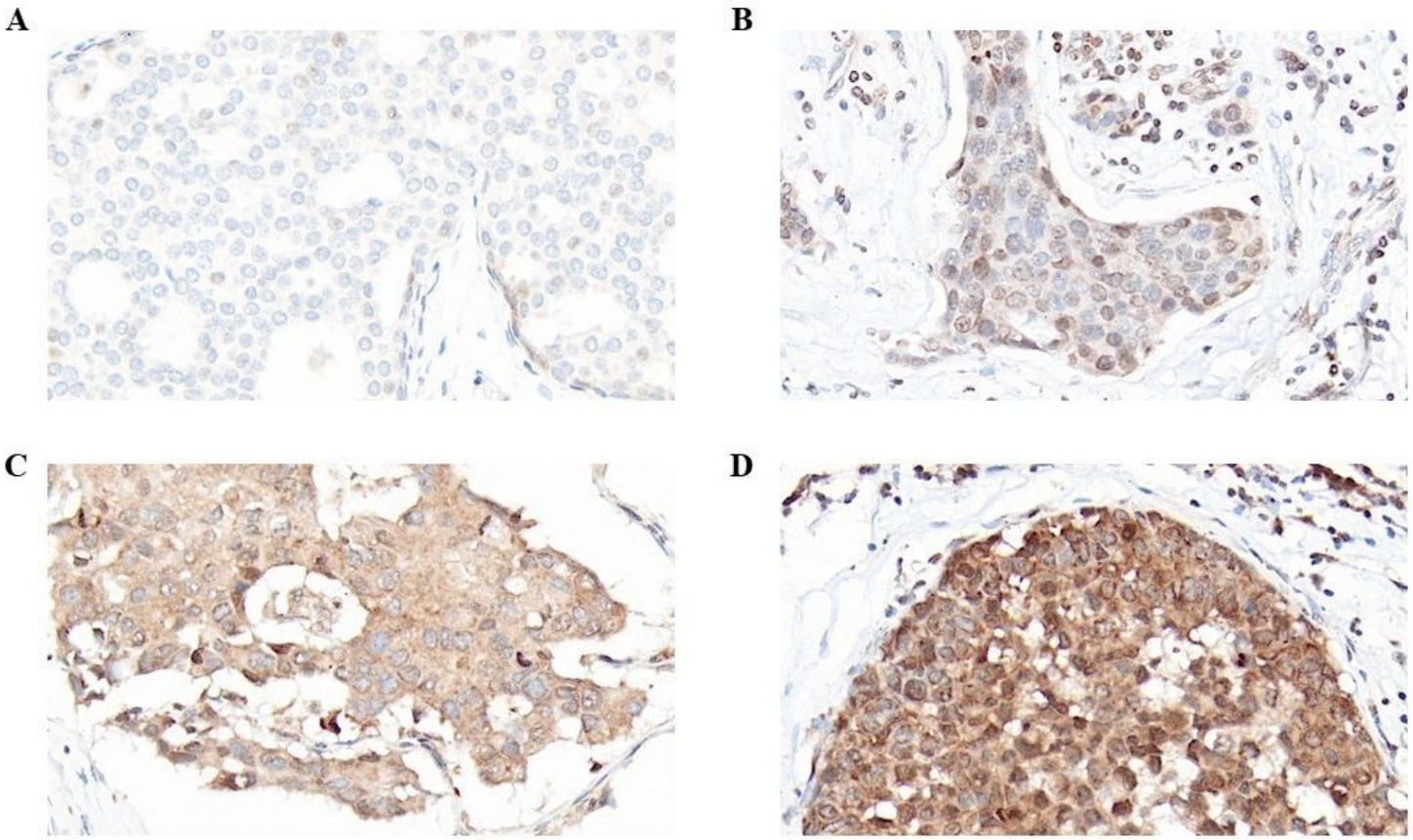

Figure 2

Representative images of ACSL3 immunohistochemical staining for each of the scores (0–3) in breast cancer tissues. Magnification×400. (A) Negative control (score = 0), (B) ACSL3 weak positive (score = 1), (C) ACSL3 moderate positive (score = 2), (D) ACSL3 strong positive (score = 3).

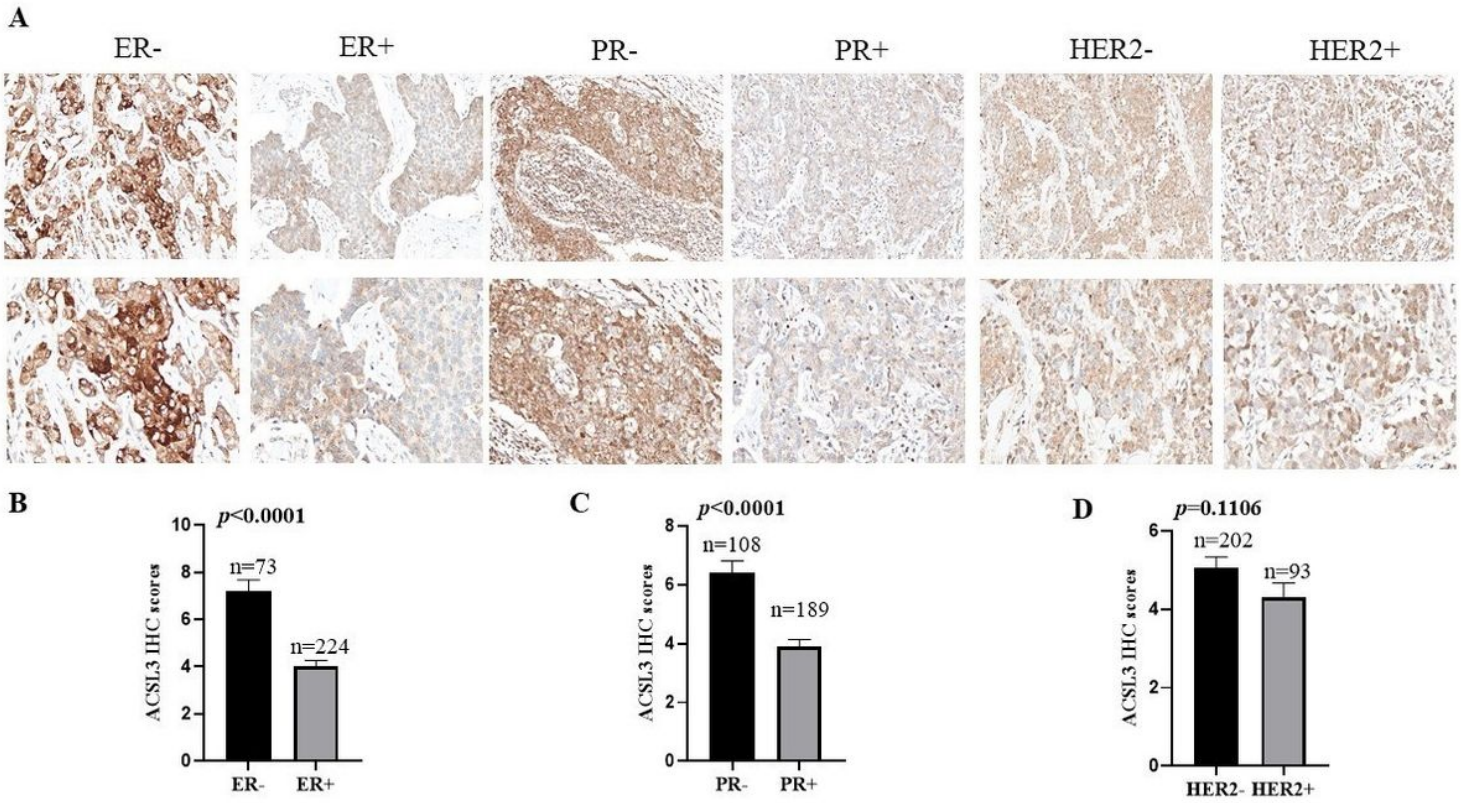

Figure 3

Evaluation of ACSL3 expression with status of ER, PR and HER2. (A) Representative images of ACSL3 immunohistochemical staining in different status of ER, PR and HER2. (B) Semi-quantitative result of ACSL3 protein expression in ER-negative and ER-positive breast tumor tissues is disclosed as the mean ± SEM. (C) Semi-quantitative result of ACSL3 protein expression in PR-negative and PR-positive breast tumor tissues is displayed as the mean ± SEM. (D) Semi-quantitative result about ACSL3 protein expression in HER2-negative and HER2-positive breast tumor tissues is displayed as the mean ± SEM.

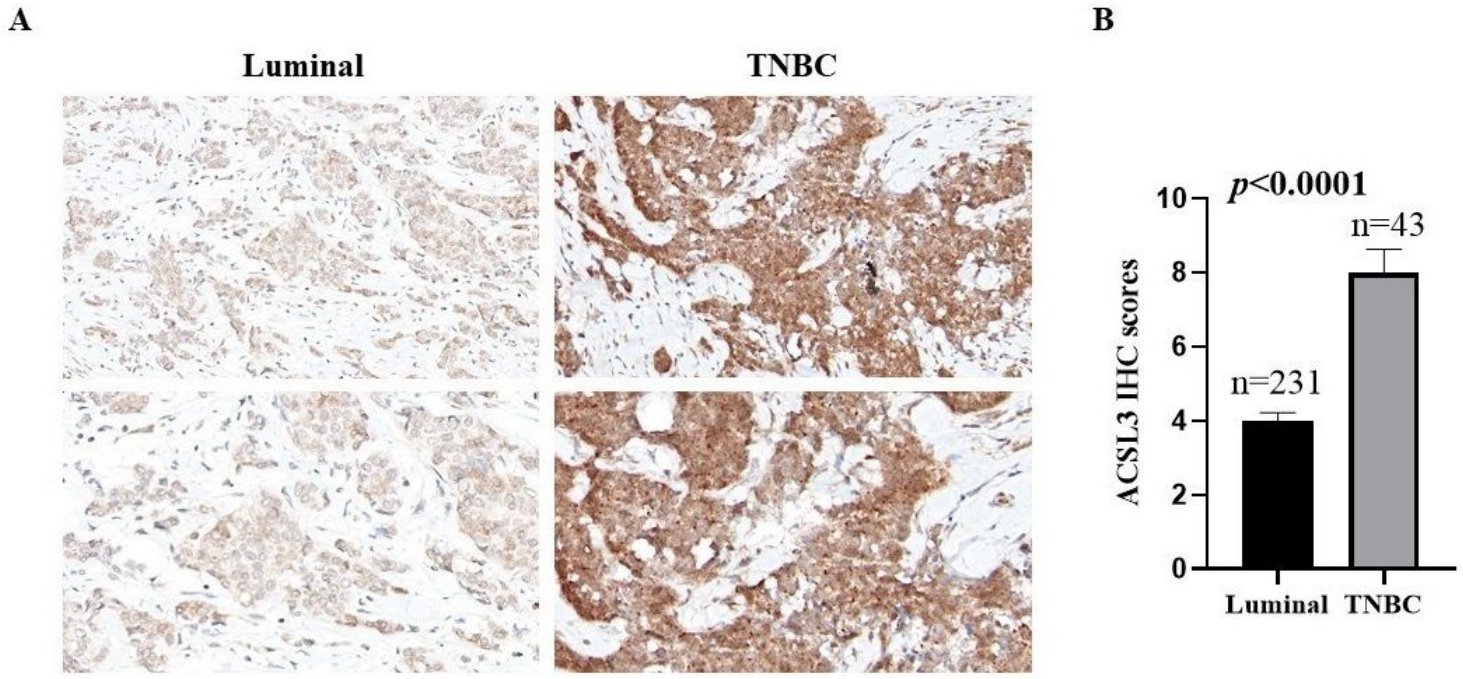

Figure 4

ACSL3 is associated with molecular subtypes of breast cancer. (A) Representative images of IHC staining for luminal-type and TNBC breast cancer tissues were showed. (B) Semi-quantitative result about ACSL3 protein expression in TNBC tissues and luminal-type breast tumor tissues is displayed as the mean ± SEM.

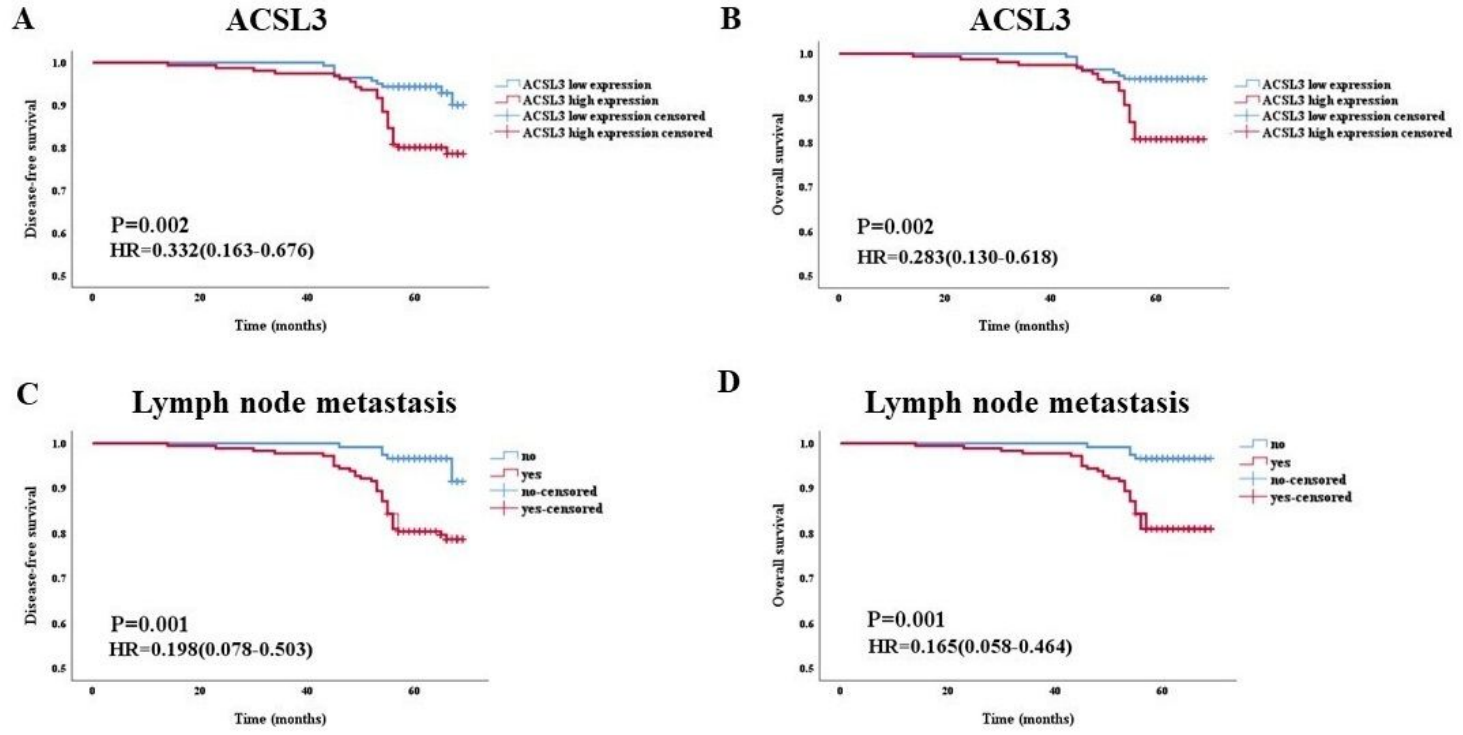

Figure 5

(A) The prognostic value of ACSL3 in patients with breast cancer for DFS. (B) The prognostic value of ACSL3 in patients with breast cancer for OS. (C)The prognostic value of lymph node metastasis in patients with breast cancer for DFS. (D)The prognostic value of lymph node metastasis in patients with breast cancer for OS.

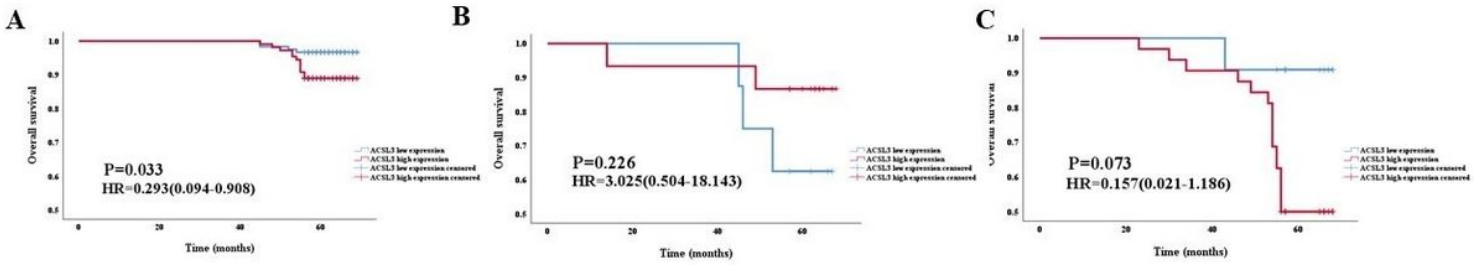

Figure 6

Kaplan-Meier survival curves for the correlation of ACSL3 protein expression with different molecule subtypes of breast cancer. The correlation between ACSL3 protein level and overall survival in luminal (A), HER2 positive (B), and TNBC (C) patients.

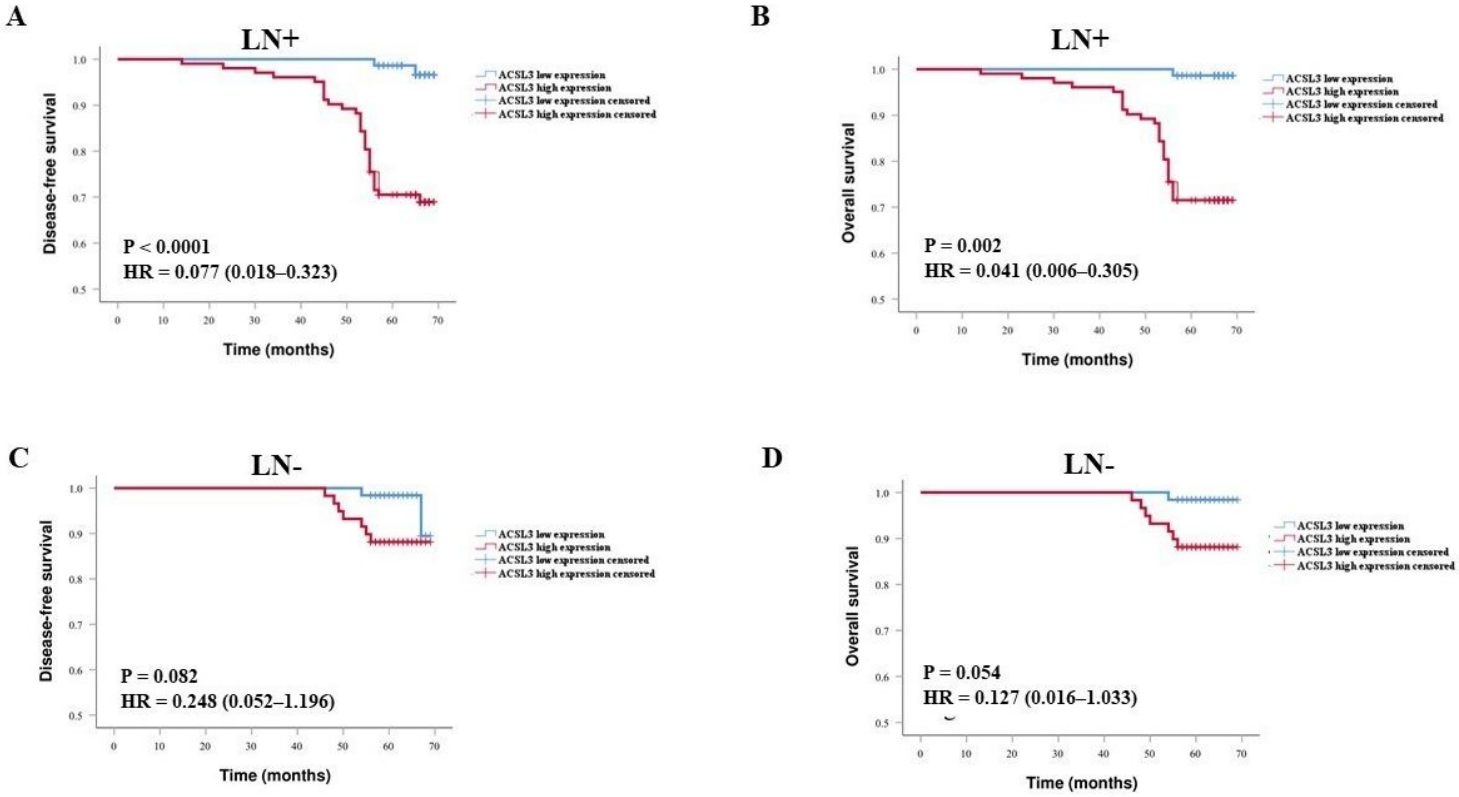

Figure 7

ACSL3 expression was an unfavorable prognostic biomarker for breast carcinoma patients with lymph node metastasis. Kaplan-Meier plotter analysis revealed that high ACSL3 protein expression was associated with poor DFS (A) and OS (B) in patients with lymph node metastasis. No significant

correlation between ACSL3 protein expression and DFS (C), OS (D) was found in patients without lymph node metastasis. LN–, lymph node metastasis negative; LN+, lymph node metastasis positive.

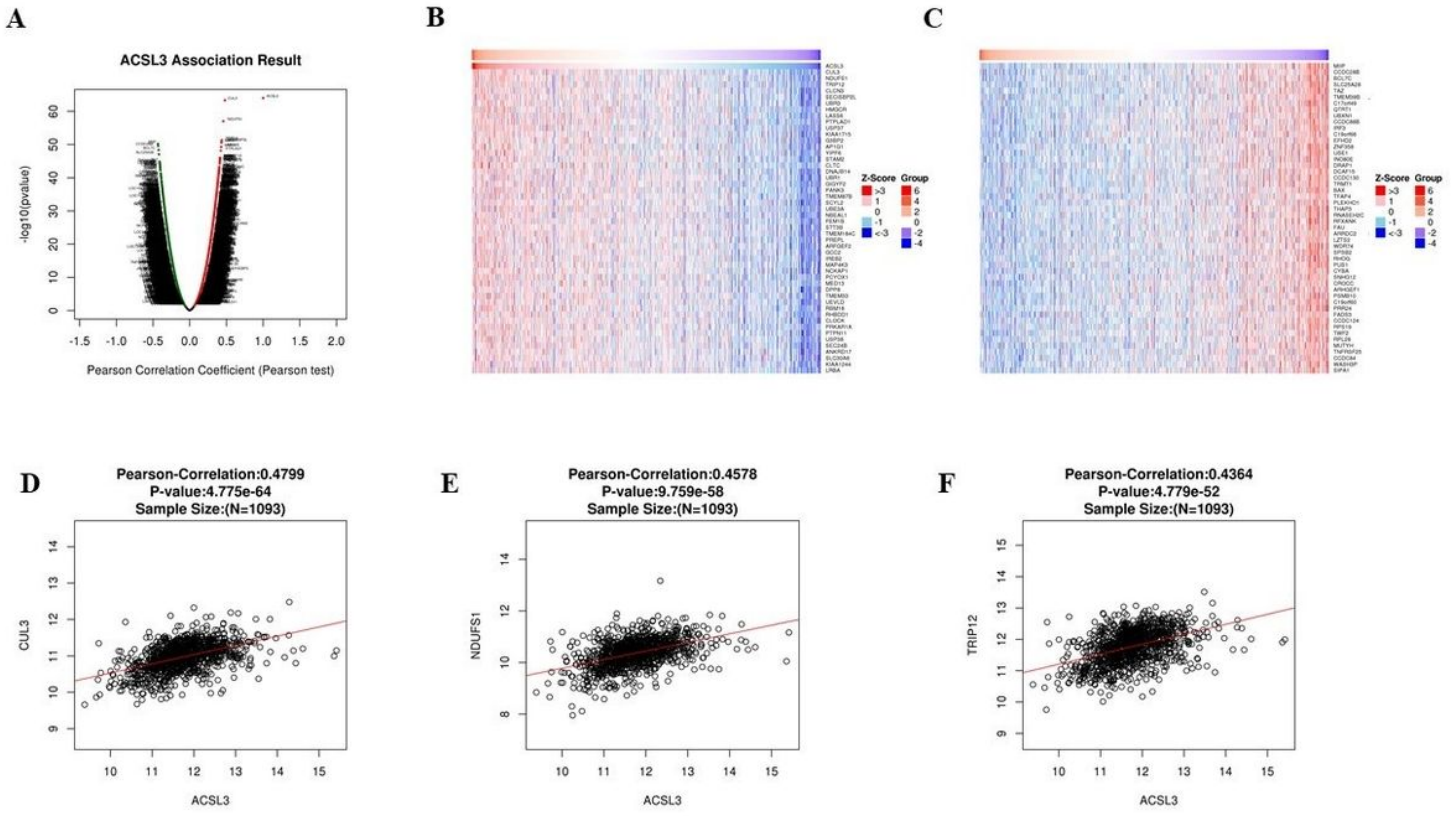

Figure 8

Genes differentially expressed in correlation with ACSL3 in breast cancer (LinkedOmics). (A) A Pearson test was used to analyze correlations between ACSL3 and genes differentially expressed in breast cancer. (B–C) Heat maps showing genes positively and negatively correlated with ACSL3 in breast cancer. Red indicates positively correlated genes and green indicates negatively correlated genes. The scatter plot shows Pearson correlation of ACSL3 expression with expression of CUL3 (D), NDUFS1 (E), and TRIP12 (F).

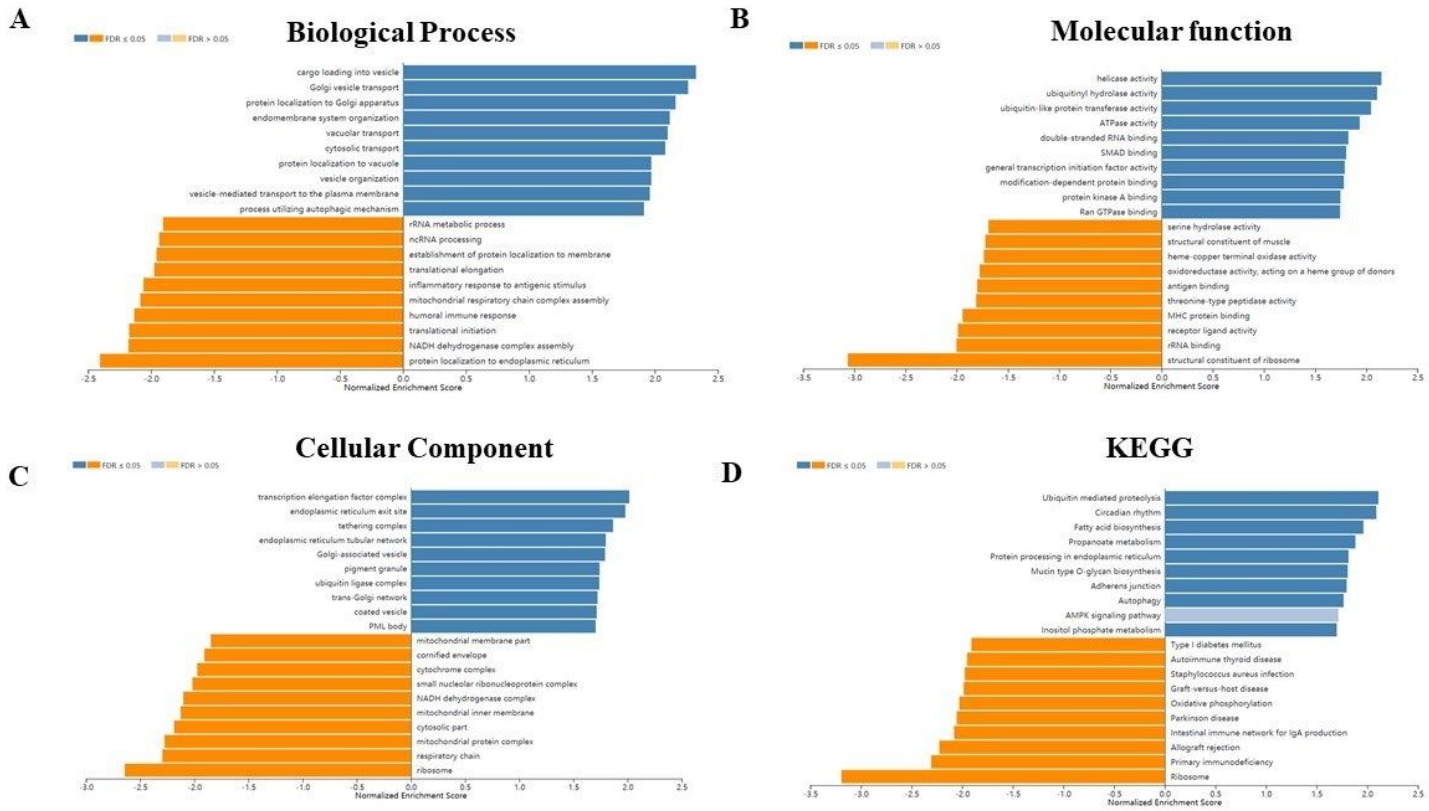

Figure 9

Significantly enriched GO annotations and KEGG pathways of ACSL3 in breast cancer. The significantly enriched GO annotations and KEGG pathways of ACSL3 co-expression genes in breast cancer were analyzed using GSEA. (A) Cellular components. (B) Biological processes. (C) Molecular functions. (D) KEGG pathway analysis.

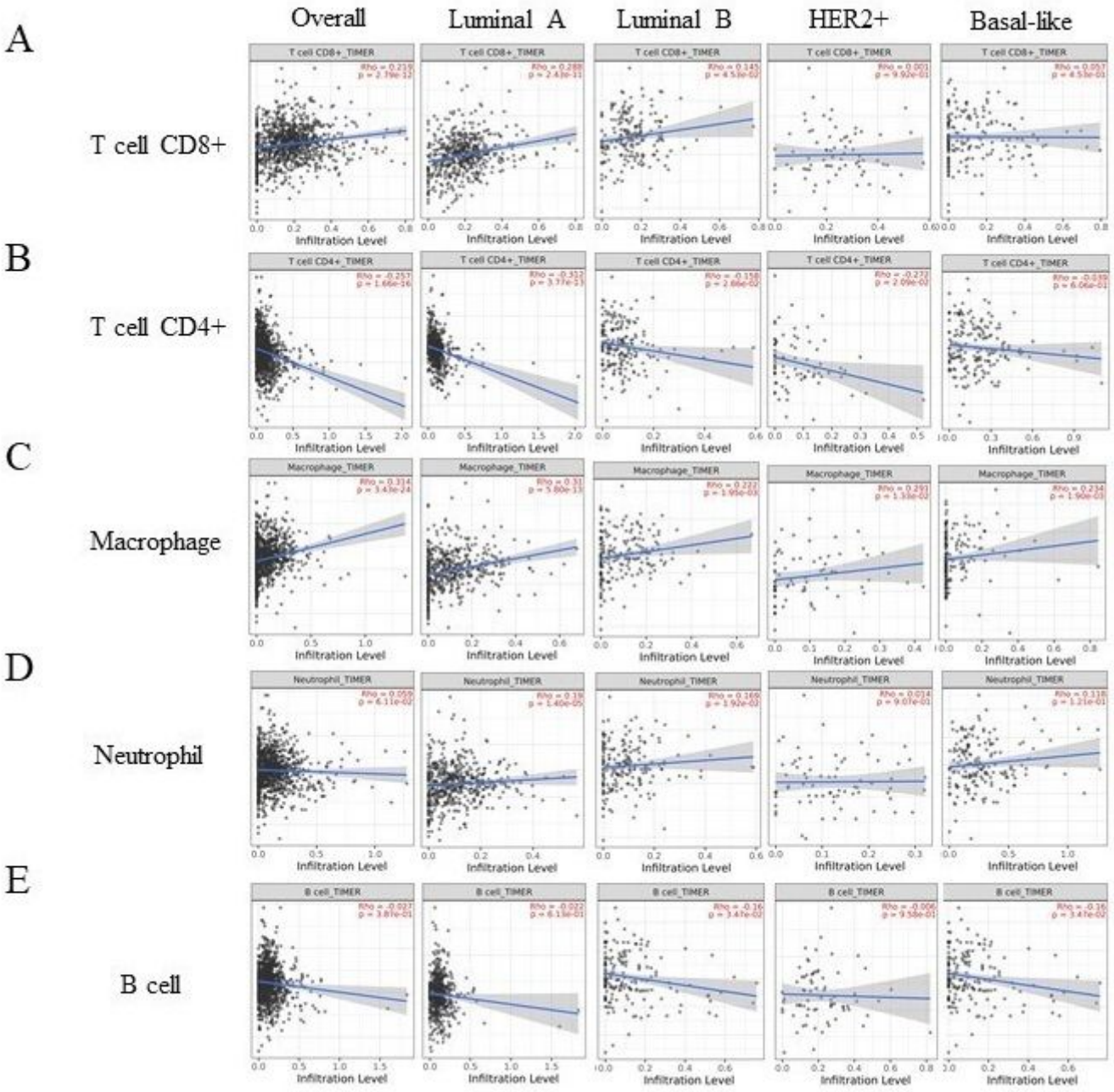

Figure 10

Correlation of ACSL3 expression with immune infiltration level in the TIMER database. Correlation of ACSL3 expression with infiltrating levels of CD8+ T cells (A), CD4+ T cells (B), Macrophage (C), Neutrophil (D) and B cell (E).